# Viscosity Effects on One-Dimensional Consolidation of Clay

Bipul C. Hawlader[1]; Balasingam Muhunthan[2]; and Goro Imai[3]

**Abstract:** A constitutive relationship for one-dimensional consolidation of clays is presented. It recognizes the importance of structural viscosity and yielding in controlling many of the phenomena associated with the consolidation of clays. The governing equation for the large strain consolidation of clays, incorporating the new constitutive relationship, has been solved using a finite difference technique. The computer program has been verified using laboratory experiments including those performed on an interconnected consolidometer. The laboratory tests and numerical results are used to examine many of the current hypotheses used in predicting field consolidation. The results show that the deformation of thick clays in the field are different from those predicted from a thin laboratory specimen using the square of the drainage length or the uniqueness of the end of primary consolidation concepts. The dominance of the structural viscosity during the primary consolidation stage has been shown to be the main source of the discrepancy.

**DOI:** 10.1061/(ASCE)1532-3641(2003)3:1(99)

**CE Database subject headings:** Consolidation; Viscosity; Yield; Void ratio; Clays

## Introduction

Consolidation settlement of clay is the combined effect of stress and time-dependent deformations. Both effects start simultaneously just after the application of load. The mechanics of the origin of the time-dependent deformation behavior is complex. Various views have been put forward in the literature about its origin (Murakami 1988). Avoiding the use of different semantics, in this study the time dependency during consolidation is assumed to be caused by the ''viscosity'' of the soil skeleton. Both hydrodynamic pore pressure dissipation and viscous effects are present in the primary consolidation, whereas only viscous effects exist in the secondary consolidation because the excess pore pressures have dissipated.

Compression due to viscous effects is most likely to be larger in the field. It is, therefore, necessary to develop a model that takes into account the viscous nature of consolidation of clays (Mitchell 1976; Leroueil et al. 1985; Crawford 1986). Taking into account the viscosity during primary consolidation, several constitutive models were developed in the past either as a function of time (e.g., Murakami 1988; Yin and Graham 1989) or as a function of strain rate ($\dot{\varepsilon}$) (e.g., Kabbaj et al. 1986). The main advantage of the later approach is that it does not require the initial time. The model developed by Kabbaj et al. (1986) does not account for the viscous behavior of clay prior to yield.

This paper presents a new constitutive model of consolidation that has been developed from the laboratory test results using an interconnected consolidometer. The model considered not only the effect of viscosity during primary consolidation but also the strain rate effects on yield resulting from the secondary compression during previous loading. Effects of self-weight and variable permeability are also taken into account in the proposed finite strain consolidation analysis. A finite-difference numerical algorithm is used to solve the governing equation of consolidation incorporating the new constitutive model.

[1]Research Engineer, C-CORE, Memorial Univ. of Newfoundland, St. John's NL, Canada A1B 3X5.

[2]Associate Professor, Civil and Environmental Engineering, Washington State Univ., Pullman, WA 99164-2910.

[3]Professor, Dept. of Civil Engineering, Yokohama National Univ., 79-5 Tokiwadai, Hodogaya-ku, Yokohama 240-8501, Japan.

Note. Discussion open until February 1, 2004. Separate discussions must be submitted for individual papers. To extend the closing date by one month, a written request must be filed with the ASCE Managing Editor. The manuscript for this paper was submitted for review and possible publication on August 16, 2001; approved on April 10, 2002. This paper is part of the ***International Journal of Geomechanics***, Vol. 3, No. 1, September 1, 2003. ©ASCE, ISSN 1532-3641/2003/1-99–110/$18.00.

## Past Works on Consolidation of Clays

The time-dependent deformation of clays has been the subject of intense investigation since the original contribution to the consolidation theory by Terzaghi (1923). Many useful concepts relating to the prediction of void ratio changes and settlement due to consolidation have been proposed. Yet important differences exist in the manner in which changes in void ratio are accounted for during the consolidation of clay. The void ratio change of a clay element during consolidation is a function of both effective stress change and time (Mesri and Choi 1979)

$$\frac{de}{dt}=\left(\frac{\partial e}{\partial \sigma'}\right)_t \frac{d\sigma'}{dt}+\left(\frac{\partial e}{\partial t}\right)_{\sigma'} \tag{1}$$

where $(\partial e/\partial \sigma')_t$ = void ratio change with respect to effective stress only, and $(\partial e/\partial t)_{\sigma'}$ = decrease in void ratio with time for a constant effective stress. The change in void ratio can be obtained by integrating Eq. (1) as

$$\Delta e=\int_0^t\left[\left(\frac{\partial e}{\partial \sigma'}\right)_t \frac{d\sigma'}{dt}+\left(\frac{\partial e}{\partial t}\right)_{\sigma'}\right]dt \tag{2}$$

In practice, however, the entire consolidation process is divided into primary and secondary consolidation stages. During primary consolidation both seepage and viscous resistance retards the transition of soil particles into a new equilibrium state under applied stress while mainly the viscous resistance is active in the secondary consolidation phase. Accordingly, Eq. (2) is evaluated by

$$\Delta e=\int_0^{t_p}\left[\left(\frac{\partial e}{\partial \sigma'}\right)_t \frac{d\sigma'}{dt}+\left(\frac{\partial e}{\partial t}\right)_{\sigma'}\right]dt+\int_{t_p}^{t}\left(\frac{\partial e}{\partial t}\right)_{\sigma'} dt \tag{3}$$

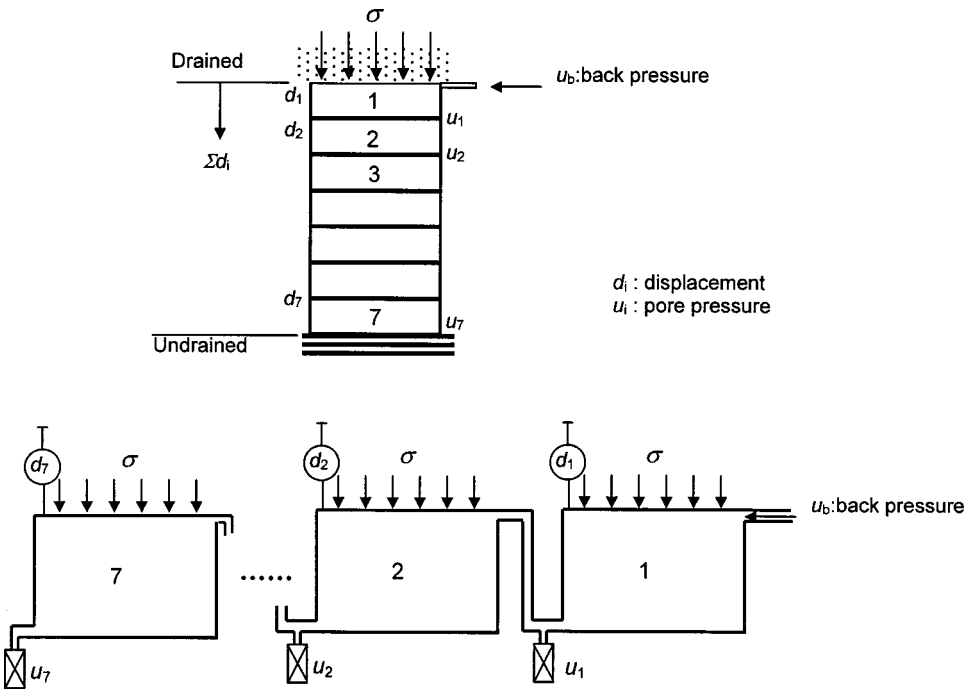


**Fig. 1.** Basic concept of interconnected consolidation test

where $t_p$ represents the duration of primary consolidation.

Based on the test results on clay specimens of different thickness, Mesri and his co-workers (Mesri and Choi 1979, 1985; Mesri et al. 1995) developed a unique end-of-primary (EOP) void ratio concept for computing primary consolidation settlement of thick clay layers in the field. However, several researchers (e.g., Aboshi 1973; Murakami 1988; Imai and Tang 1992) reported that the strain at the EOP consolidation increases with the thickness of specimen. The presence of viscous effects during primary consolidation was suggested as the main cause for the nonuniqueness of EOP strain.

It has also been observed that a clay specimen allowed to consolidate for a long time after the primary consolidation behaves as if it had a quasipreconsolidation pressure that is greater than the initial consolidation pressure during subsequent loading (Leonards and Altschaeffl 1964; Murakami 1988). In this study, following Leroueil (1997), it is preferred to term the quasipreconsolidation stress as a yield stress that separates small and large deformation during consolidation. This yield stress is significant to geotechnical practice, but many engineers are still uncertain of its magnitude and the manner in which to incorporate it in consolidation analysis. Mesri and Choi (1979) and Murakami (1992) proposed some empirical relationships to compute this yield stress. It will be shown later that this yield stress is a function of strain rate (or void-ratio rate), which is not accounted for in these empirical relations.

## Consolidation of Clay with Drainage Distance

Imai (1995) developed an interconnected consolidometer to examine the consolidation behavior of clay elements located at different drainage distances. This device consists of seven subcells of 60 mm i.d. and 5 mm height as shown schematically in Fig. 1. Drainage was provided only at the top of the cell arrangement. The subspecimens were connected to enable a continuous flow of pore water. Additional details of the test and the method of sample preparation have been provided by Imai (1995).

When a consolidation pressure $\sigma$ is applied at the top of the consolidometer, each subspecimen begins to consolidate. The displacement $(d_i)$ and pore water pressure $(u_i)$ for each subspecimen is measured with time. These measurements are used to calculate the change in effective stress $(\Delta\sigma')$ and void ratio $(\Delta e)$ for the total specimen and subspecimens.

A series of consolidation tests were performed on reconstituted soil samples prepared from Yokohama Bay Mud using this device. The preconsolidation pressure of all the samples was 0.5 kg/cm$^2$. The typical void ratio change for a load increment within each subspecimen is shown in Fig. 2(a). It shows that the state path $(e-\log\sigma')$ for each subspecimen is different and is dependent on the distance from the drainage boundary. It also shows that the change in void ratio with increase in effective stress is small at the initial stage for all subspecimens. This is followed by a rapid reduction in void ratio after some stress level clearly depicting the presence of yield.

The void-ratio-rate $(\dot{e}=-\Delta e/\Delta t=-(e_i-e_f)/\Delta t)$ during consolidation of subspecimens is dependent both on its state of effective stress and the distance from the drainage face. The variation of void-ratio-rate for different load increment ratios (LIRs) (0.8→2.4 kg/cm$^2$;0.8→3.2 kg/cm$^2$;1.6→3.2 kg/cm$^2$;2.4→4.8 kg/cm$^2$) is shown in Fig. 2(b). It can be seen that despite the use of different LIRs, the void-ratio-rate lines are parallel to each other. The slope of these lines was found to be approximately equal to the compression index $C_c$ in an $e-\log\sigma'$ plot (Imai 1995).

Fig. 2(c) shows a plot of void-ratio-rate against the specific parameter $\Gamma(=e+C_c\log\sigma'$; where $\sigma'$ is in kg/cm$^2$), proposed by Hawley and Borin (1973). Here $\Gamma$ is a parameter that defines the relative position of the current state of a soil element $(e,\sigma')$ measured from the basic compression line which passes through the initial state point $(e_0,\sigma'_0)$ [point A in Fig. 3(b)] and having the slope $C_c$ (Hawley and Borin 1973). The solid lines in Fig. 2(c)

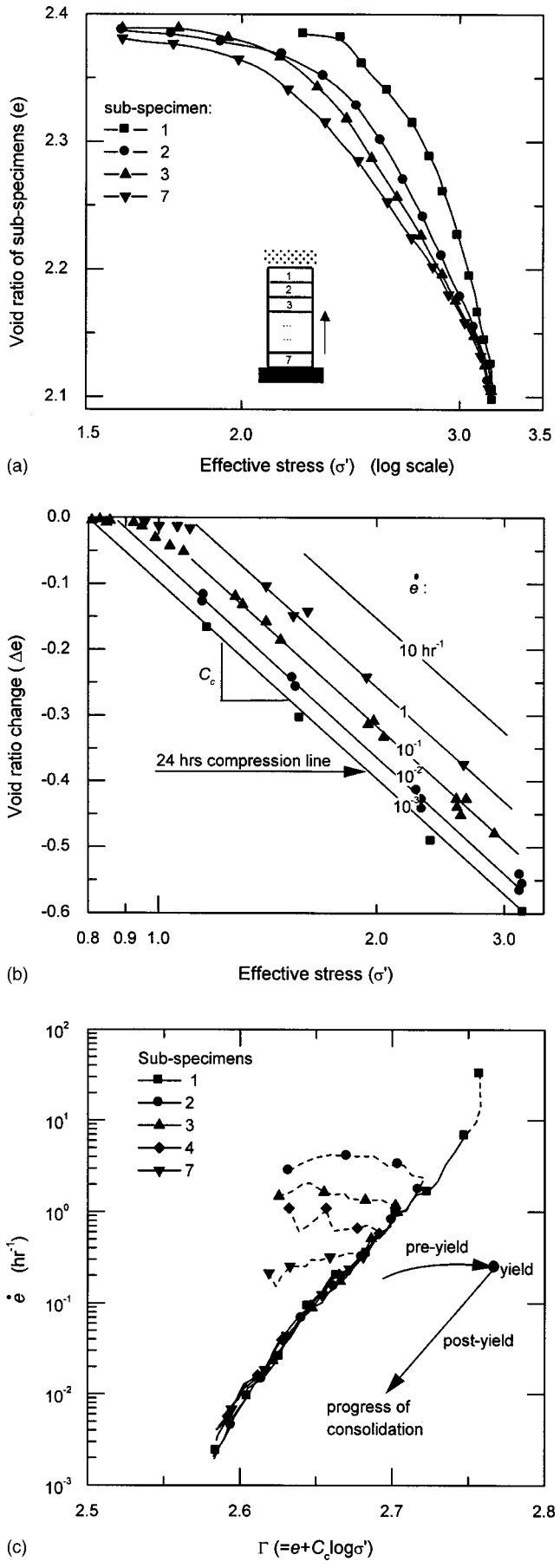


**Fig. 2.** (a) State path ($e-\log\sigma'$) of subspecimens; (b) void-ratio-rate lines; and (c) relationship between $\Gamma$ and $\dot{e}$

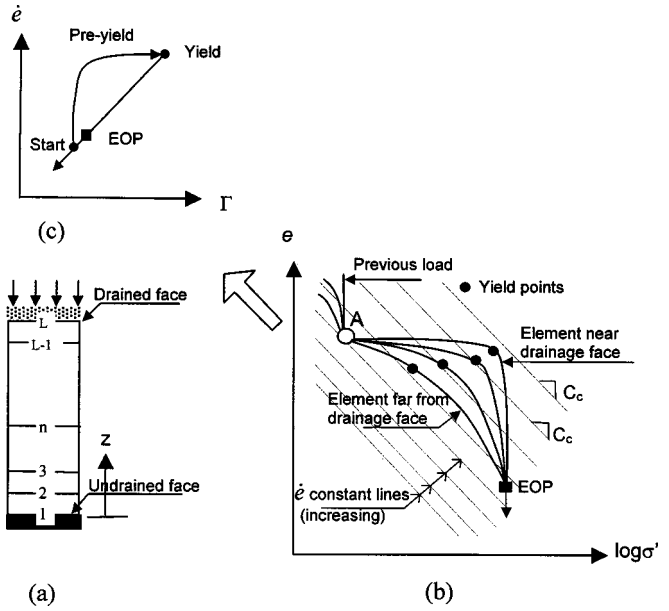


**Fig. 3.** Proposed consolidation model

denote the post-yield changes in void-ratio-rate of sub-specimens with $\Gamma$. As shown in this figure, a unique linear relationship can represent the change in void-ratio-rate with $\Gamma$ of all the subspecimens irrespective of their location

$$\Gamma = s\log(-\dot{e}) + b \tag{4}$$

The soil parameters $s$ and $b$ can be obtained from a one-dimensional consolidation test (Imai 1995). The parameter $s$ is related to the structural viscosity of the clay skeleton. In fact, experimental results show that $s$ is approximately equal to the coefficient of secondary compression, $C_\alpha$ (Imai and Tang 1992, Imai 1995).

Imai (1995) also showed that if the total void ratio change is separated into its recoverable ($\Delta e^r$) and irrecoverable ($\Delta e^{ir}$) components then the latter ($\Delta e^{ir}$) can be represented by a relation similar to Eq. (4)

$$e^{ir} + C_c\log\sigma' = C_\alpha\log(-\dot{e}^{ir}) + b \tag{5}$$

## Proposed Consolidation Model

The above observations on the distinct consolidation behavior of elements with respect to their drainage distance have been used to formulate a constitutive model. The underlying ideas of the proposed model are shown schematically in Fig. 3(b). The inclined parallel dotted lines in this figure are the void-ratio-rate ($\dot{e}$) lines, which also represent the time effects on consolidation. Suppose a clay specimen begins to consolidate from an initial state A [Fig. 3(b)]. If the applied stress is larger than the yield stress, the specimen will first experience some void ratio change caused by the initial nonlinear elastic deformation followed by postyield deformation governed by Eq. (4). In order to determine the state of yield, we form

$$\Delta f = [e + C_c\log\sigma'] - [C_\alpha\log(-\dot{e}) + b] \tag{6}$$

The value of $\Delta f$ is calculated for each time step by using the current values $(e,\sigma',\dot{e})$. The first [ ] term on the right hand side of Eq. (6) is the current value of $\Gamma$ before yield and the second [ ] term is the expected value of $\Gamma$ if the soil element is in a state of

complete yield with respect to the current value of $\dot{e}$. The magnitude of $\Delta f$ is then a measure of the closeness of the state of a soil element that is to yield. Its value is zero when an element yields.

Note that the rate of compression for each element within the clay layer is different, since compression is associated with the expulsion of pore water and viscosity. The pore water pressure dissipation depends on the drainage distances ($z$) [see Fig. 3(a)]. Therefore, for elements near the drainage boundary effective stresses will increase rapidly and their compression curves will experience higher void-ratio rates. However, pore pressures will dissipate slowly for elements away from the drainage boundaries. Consequently, the compression of these elements will be delayed before reaching the same level of effective stress as an element near the drainage boundary. Therefore, the state path of elements at larger distances from the drainage boundaries will follow further down in the system of parallel ($-\dot{e}$) lines than those elements at shorter distances from the drainage boundary in an effective stress versus void ratio plot. Notice that the points of yield, denoted by solid circles [Figs. 3(b and c)], are also dependent on the drainage distance in addition to the secondary compression that occurred under previous loading. The yield stress is higher for an element near the drainage boundary. Moreover, the larger the amount of secondary consolidation during the previous load increment the higher is its yield stress.

## Void Ratio Changes

The deformation of a clay element consists of elastic component that is recoverable upon unloading and visco–plastic component that is irrecoverable. Therefore, the total change in void ratio ($\Delta e$) of a consolidating soil element is separated into two components; recoverable ($\Delta e^r$) and irrecoverable ($\Delta e^{\text{ir}}$). The recoverable component can be obtained as

$$-\Delta e^r = C_s \Delta \log \sigma' = 0.434 C_s \frac{\Delta \sigma'}{\sigma'} \tag{7}$$

where $C_s$ = swelling index. Since the initial portion of the void ratio curve is nonlinear elastic and dependent on viscosity, the change in void ratio prior to the yield is calculated by a slightly modified form of Eq. (7)

$$-\Delta e = 0.434 C_t \Delta \sigma'/\sigma' \tag{8}$$

where

$$C_t = C_s + \frac{C_c - C_s}{1+\mu \Delta f}$$

Based on a best-fit approximation for the preyield consolidation process, a value of $\mu = 100$ is used in this study. It will be shown later that the use of $\mu$ in $C_t$ enables a gradual change in compressibility from preyield to postyield consolidation conditions. Note that $\mu$ is dependant on the mechanical properties of the soil.

The irrecoverable component, ($\Delta e^{\text{ir}}$), occurs after yielding and consists of plastic and viscous parts. Since $\dot{e}^{\text{ir}}$ is a function of $\sigma'$ and $e^{\text{ir}}$ [Eq. (5)], using the chain rule

$$\Delta(-\dot{e}^{\text{ir}}) = f_{\sigma'} \Delta \sigma' + f_{e^{\text{ir}}} \Delta e^{\text{ir}} \tag{9}$$

where

$$f_{e^{\text{ir}}} = \frac{-\dot{e}^{\text{ir}}}{0.434 C_\alpha}, \quad f_{\sigma'} = \frac{C_c}{C_\alpha} \frac{-\dot{e}^{\text{ir}}}{\sigma'}$$

The average void-ratio rate ($-\dot{e}^{\text{ir}}_{\text{av}}$) between time $t$ and $t+\Delta t$ is

$$-\dot{e}^{\text{ir}}_{\text{av}} = (-\dot{e}^{\text{ir}}) + \Delta(-\dot{e}^{\text{ir}})/2 \tag{10}$$

Using $\Delta e^{\text{ir}} = \dot{e}^{\text{ir}}_{\text{av}} \Delta t$, a relationship among $\Delta e^{\text{ir}}$, $\Delta \sigma'$, and $\Delta t$, can be established as

$$-\Delta e^{\text{ir}} = \frac{f_{\sigma'} \Delta t}{2 + f_{e^{\text{ir}}} \Delta t} \Delta \sigma' - \frac{2 \dot{e}^{\text{ir}} \Delta t}{2 + f_{e^{\text{ir}}} \Delta t} \tag{11}$$

The total void ratio change $\Delta e$ during postyield consolidation is obtained by combining Eqs. (7) and (11)

$$-\Delta e = -(\Delta e^r + \Delta e^{\text{ir}}) = A_1 \Delta \sigma' + B_1 \Delta t \tag{12}$$

where,

$$A_1 = 0.434 \frac{C_s}{\sigma'} + \frac{f_{\sigma'} \Delta t}{2 + f_{e^{\text{ir}}} \Delta t}$$

and

$$B_1 = \frac{-2 \dot{e}^{\text{ir}}}{2 + f_{e^{\text{ir}}} \Delta t}$$

For preyield consolidation, $A_1 = 0.434 C_t/\sigma'$ and $B_1 = 0$ [Eq. (8)].

## Governing Equations

The detailed development of the governing equation of large strain consolidation has been presented elsewhere (Gibson et al. 1967; Imai 1995) and will only be reviewed briefly here. The Eulerian coordinate system is usually used in most of the geotechnical infinitesimal strain problems. However, if the deformation is large compared with the thickness of the clay layer a reduced coordinate system ($z$) is convenient for consolidation analysis (Gibson et al. 1967).

$$z = \int_0^a \frac{1}{1+e_0(a)} da \tag{13}$$

where $e_0$ = void ratio at time $t=0$ and $a$ represents the Lagrangian coordinate system. The coordinate $z$ is independent of time and represents the thickness of the soil particles lying between the datum plane and the point being analyzed.

The volume reduction of a soil element during consolidation is the resultant effect of its inflow and outflow of water. Therefore, the continuity condition of a soil element can be written as (Gibson et al. 1967; Tan and Scott 1988; Imai 1995)

$$\frac{\partial v}{\partial z} + \frac{\partial e}{\partial t} = 0 \tag{14}$$

where $v$ = discharge velocity and is defined as

$$v = \frac{e(v_f - v_s)}{1+e} \tag{15}$$

$v_f$ and $v_s$ = velocities of pore water and soil skeleton, respectively. The discharge velocity ($v$) is related to hydraulic gradient ($i$) according to Darcy's law as

$$v = k_v i \tag{16}$$

where $k_v$ = coefficient of vertical permeability.

Using equilibrium of forces acting on the soil element, it can be shown that (Gibson et al. 1967; Imai 1995)

$$i = \frac{1}{\gamma_w} \left( \frac{1}{1+e} \frac{\partial \sigma'}{\partial z} + \frac{\gamma_s - \gamma_w}{1+e} \right) \tag{17}$$

where $\gamma_s$ and $\gamma_w$ = unit weight of solids and water, respectively.

Combining Eqs. (14), (16), and (17) leads to the following governing differential equation of consolidation:

$$-\frac{\partial e}{\partial t}=\alpha\left[\frac{\partial^2\sigma'}{\partial z^2}+\beta\left\{\frac{\partial\sigma'}{\partial z}+\gamma'\right\}\right] \tag{18}$$

where

$$\alpha=\frac{1}{1+e}\frac{k_v}{\gamma_w};\quad \beta=\left(\frac{1}{0.434C_k}-\frac{1}{1+e}\right)\frac{\partial e}{\partial z}$$

and

$$\gamma'=\frac{\gamma_s-\gamma_w}{1+e}$$

The coefficient of vertical permeability ($k_v$) is assumed to be a function of void ratio (Tavenas et al. 1983; Imai and Tang 1992)

$$\log k_v=\log k_{v0}-\frac{e_0-e}{C_k} \tag{19}$$

where $k_{v0}$=coefficient of permeability at initial void ratio ($e_0$); and $C_k$=permeability change index ($\approx 0.5e_0$), (Tavenas et al. 1983).

## Numerical Implementation

The governing equation of consolidation has been solved using the finite difference technique. The vertical position of the grid point is denoted by the subscript $n$, while for time the superscript $k$ is used.

Using the value of $\Delta e$ from Eq. (12) and applying central difference approximation to Eq. (18) at a grid point $n$ at time step $k$, leads to

$$\frac{\sigma_n'^{k+1}-\sigma_n'^{k}}{\Delta t}=\Lambda(\sigma_{n+1}'^{k}) \tag{20}$$

where $\Lambda(\sigma_{n+1}'^{k})$ is the difference operator that results from central difference approximation

$$\Lambda(\sigma_{n+1}'^{k})=P\sigma_{n+1}'^{k}+Q\sigma_n'^{k}+R\sigma_{n-1}'^{k}+S \tag{21}$$

in which

$$P=\frac{\alpha}{A_1(z_{n+1}-z_{n-1})}\left(\frac{1}{z_{n+1}-z_n}+\beta\right)$$

$$Q=-\frac{\alpha}{A_1(z_{n+1}-z_{n-1})}\left(\frac{1}{z_{n+1}-z_n}+\frac{1}{z_n-z_{n-1}}\right)$$

$$R=\frac{\alpha}{A_1(z_{n+1}-z_{n-1})}\left(\frac{1}{z_n-z_{n-1}}-\beta\right)$$

$$S=\frac{\alpha\beta\gamma'}{A_1}-B_1$$

Recall that $A_1$ and $B_1$ are the parameters that account for the effect of viscosity in the set of finite difference equations above [see also Eq. 12].

The finite difference form of the governing equation [Eq. (20)] is solved numerically using the Crank–Nicolson's scheme (Thomas 1995). Use of this scheme has been shown to provide not only a computationally efficient implicit scheme but also to guarantee its stability (Thomas 1995). The Crank–Nicholson scheme utilizes the time averages of the difference operator between the grid points $k$ and $k+1$. Accordingly, Eq. (20) becomes

$$\sigma_n'^{k+1}-\tfrac{1}{2}[\Lambda(\sigma_{n+1}'^{k+1})]\Delta t=\sigma_n'^{k}+\tfrac{1}{2}[\Lambda(\sigma_{n+1}'^{k})]\Delta t \tag{22}$$

The above equation leads to a tridiagonal matrix system of equations for the new values of $\sigma_{n-1}'^{k+1}$, $\sigma_n'^{k+1}$, and $\sigma_{n+1}'^{k+1}$ as

$$C_{1,n}\sigma_{n-1}'^{k+1}+C_{2,n}\sigma_n'^{k+1}+C_{3,n}\sigma_{n+1}'^{k+1}=C_{4,n} \tag{23}$$

where

$$C_{1,n}=-P\Delta t/2$$

$$C_{2,n}=(1-Q\Delta t/2)$$

$$C_{3,n}=-R\Delta t/2$$

$$C_{4,n}=\sigma_n'^{k}+[P\sigma_{n+1}'^{k}+Q\sigma_n'^{k}+R\sigma_{n-1}'^{k}+2S]\Delta t/2$$

The constants $C_{i,n}$ [$i=1,2,3,4$ in Eq. (23)] are calculated at the grid points along $z$ ($n=2,3,4,..L-1$) during computation [Fig. 2(a)]. Incorporating the boundary conditions for the first and the last nodes (i.e., nodes 1 and $L$) as described later, the simultaneous equations [Eq. (23)] for different nodes are then solved to obtain $\sigma^{k+1}$. The computation then shifts to the next time step and the process is repeated. A complete listing of the computer code that was used in the analyses can be found in Hawlader (1998). The details of the analysis made to ensure the stability of the solution have also been presented there.

## Boundary Conditions

### *Drained Surface*

The presence of a fully pervious material at the top of the clay layer will result in the complete dissipation of pore pressure immediately after the application of load. Therefore, the reduction of void ratio of an element at this boundary for subsequent time increments will be only a function of time governed by Eq. (5) without any stress increment (i.e., $\Delta\sigma'=0$, $\Delta e=\Delta e^{\text{ir}}$, and $\dot{e}=\dot{e}^{\text{ir}}$).

For the time steps $k$ and $k+1$

$$\Delta e=\frac{\dot{e}^k+\dot{e}^{k+1}}{2}\Delta t/2=C_\alpha\log\left(\frac{\dot{e}^{k+1}}{\dot{e}^k}\right)=0.43C_\alpha\frac{\dot{e}^{k+1}-\dot{e}^k}{\dot{e}^k} \tag{24}$$

Eq. (24) can be rearranged as

$$\dot{e}^{k+1}=\dot{e}^k+\frac{2(\dot{e}^k)^2\Delta t}{0.868C_\alpha-\dot{e}^k\Delta t} \tag{25}$$

Once the void-ratio rate is known, $\Delta e$ can be calculated using the following relationships:

$$\Delta e=\frac{\dot{e}^k+\dot{e}^{k+1}}{2}\Delta t \tag{26}$$

### *Undrained Surface*

Along the undrained surface [i.e., at the grid point 1 in Fig. 3(a)] the flow velocity $v$ is zero throughout consolidation. Therefore, from Eqs. (16) and (17)

$$\left.\frac{\partial\sigma'}{\partial z}\right|_1=-(\gamma_s-\gamma_w) \tag{27}$$

The finite difference approximation of the above relation leads to

$$\sigma_1'=\sigma_2'+(z_2-z_1)(\gamma_s-\gamma_w) \tag{28}$$

It is noted that the pore pressure gradient is very high near a drained surface immediately after the application of a load. Ac-

cordingly, the initial time step of the calculation should be kept small enough to achieve an accurate solution. With increase in time the pore pressure distribution becomes continuous and flatter, and larger time steps can be used in the calculation (Scott 1963). Therefore, in the present study, the initial time step of 1 s is used and it is advanced according to the function $\Delta t^k = 1.005 * \Delta t^{k-1}$.

## Degree of Consolidation

Two methods are widely used to define the average degree of consolidation. The first one ($U_{\sigma'}$), is based on excess pore water pressure

$$U_{\sigma'} = 1 - \frac{\int u(z,t)dz}{\int u_0 dz} \tag{29}$$

where $u_0$ and $u$ = initial excess pore water pressure and the excess pore water pressure at time $t$, respectively.

The second definition ($U_\varepsilon$) is based on the settlement attained by the clay layer

$$U_\varepsilon = S_t / S_T \tag{30}$$

where, $S_T$ and $S_t$ = final settlement and settlement at time $t$, respectively. For a simple case where a linear stress–strain relation and a constant permeability are assumed (Terzaghi 1923), the degree of consolidation expressed in terms of excess pore water pressure is equal to that expressed in terms of settlement. However, as a result of yield and the presence of viscosity the compression behavior of clays is nonlinear and the equality does not hold.

In order to examine the effect of nonlinearity only due to yield the simple bilinear relations in the $e - \log \sigma'$ plot shown in the inset of Fig. 4 are used. The formation of yield stress is assumed to occur at the same strain level (Leonards 1985) for simplicity.

The computer program was used to analyze the consolidation behavior of a 2 cm thick soil specimen that was loaded from 0.8 to 3.2 kg/cm$^2$. Four different cases, namely, (1) no yield, (2) yield stress at 1.5 kg/cm$^2$, (3) 2.0 kg/cm$^2$, and (4) 2.5 kg/cm$^2$ were used in the numerical analysis. The average degree of consolidation predicted by Eqs. (29) and (30) is shown in Fig. 4.

It is evident that the presence of yield leads to faster pore pressure dissipation and consequently a higher degree of consolidation defined in terms of excess pore pressure ($U_{\sigma'}$) as shown in Fig. 4(a). On the contrary, the average degree of consolidation defined in terms of deformation ($U_\varepsilon$) is retarded by the presence of yield [Fig. 4(b)]. Therefore, as a result of nonlinearity, it is not possible to relate the degrees of consolidation calculated from pore pressure and that from settlement. They need to be evaluated separately.

## Comparison between Terzgahi's and Proposed Consolidation Models

Fig. 5 shows the one-dimensional consolidation test results on Yokohama clay. The specimen was initially consolidated to 0.98 kg/cm$^2$ with 24 h of consolidation for each increment using LIR = 1. Subsequently, the load on the specimen was increased to 1.96 kg/cm$^2$ and the consolidation behavior was monitored. Fig. 5 shows the laboratory test results along with predictions using the

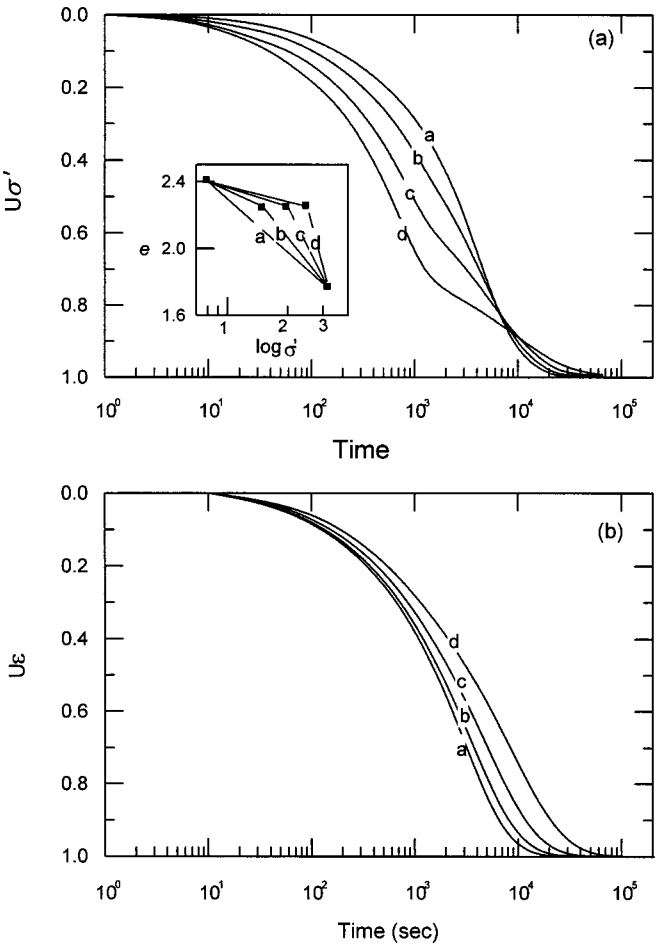


**Fig. 4.** Effect of stress–strain relation on degree of consolidation

present model and Terzaghi's one-dimensional consolidation model. The soil parameters used in this analysis are listed in Table 1. It can be seen that the strains predicted by both models match the experimental results well initially. However, near the final stage of consolidation strain ceases to develop in Terzaghi's solution whereas in the test and numerical prediction using present model the development of strain continues. Since the present model considers the consolidation phenomenon (primary and secondary) as a continuous process, it captured the continued strain development as observed in the laboratory. In other words, viscous effects contribute to the strain development even when the excess pore pressure is completely dissipated. The void-ratio rate [Fig. 5(b)] match reasonably well at the beginning but drastically reduces to zero at the end in Terzaghi's solution.

The better performance of present model over Terzaghi's model in the prediction of the excess pore pressure dissipation at the base of the specimen is evident in Fig. 5(c). The pore pressure dissipation predicted by the Terzaghi's model is remarkably slow at the initial stages of the consolidation whereas the laboratory tests and the present model indicate faster pore pressure dissipation. The faster pore pressure dissipation at the initial stage of consolidation is due to the presence of yield [cf. Fig. 4(a)]. Similar behavior was found for other load increment ratios (Hawlader 1998).

## Prediction of Strain in Field and End of Primary Strain

Numerical analyses have also been performed to study the effects of soil layer thickness on consolidation. The analyses were done

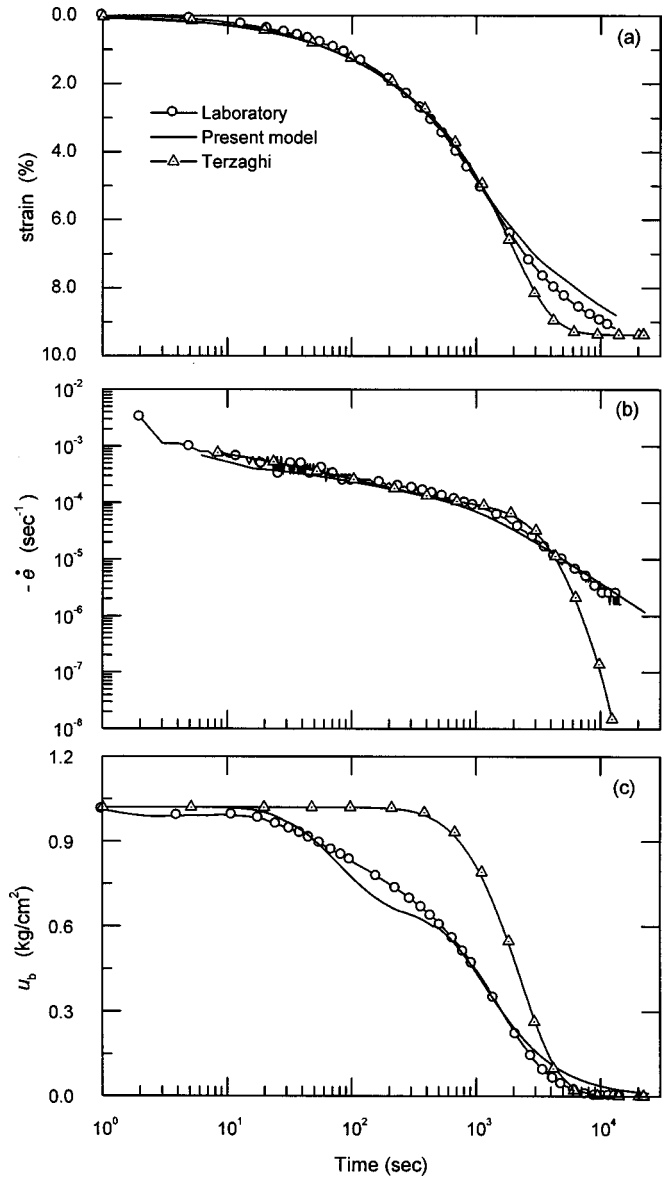


**Fig. 5.** Comparison between test results and numerical analyses

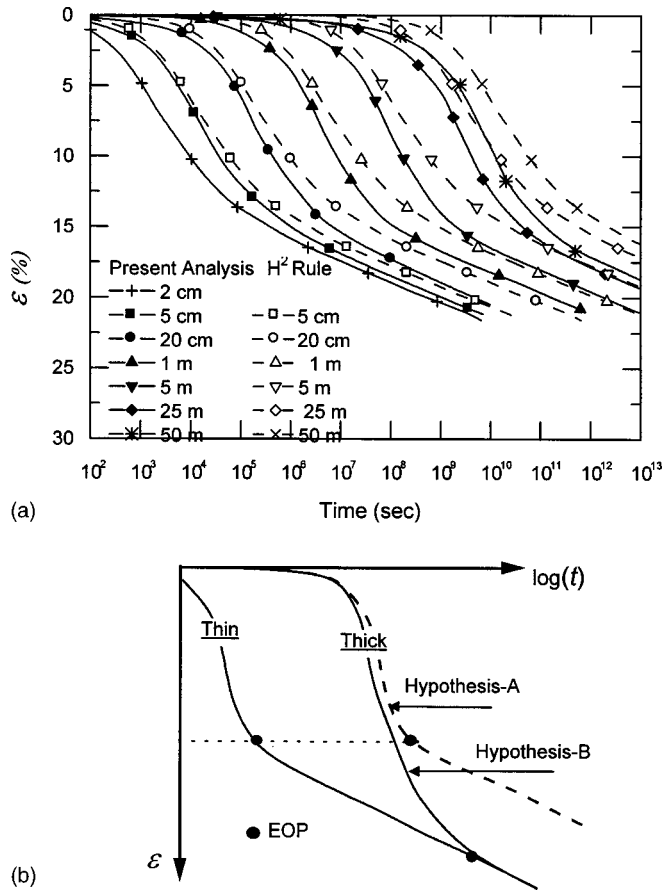


**Fig. 6.** (a) Effect of soil layer thickness on consolidation; and (b) hypothesis A and B (after Jamiolkowski et al. 1985)

for soil specimens of thickness 2 cm, 5 cm, 20 cm, 1 m, 5 m, 25 m, and 50 m with single drainage at the top. Each of these specimens is assumed to have the same sedimentation history followed by consolidation under the load of 0.8 kg/cm$^2$. The pressure was then increased from 0.8 to 3.2 kg/cm$^2$. The other input parameters used in the analyses are listed in Table 1. The predicted strain–time curves are shown in Fig. 6(a).

**Table 1.** Parameters used in Computation

| Parameters | Values |
|---|---|
| $C_s$ | 0.11 |
| $C_c$ | 1.05 |
| $C_\alpha$ | 0.05 |
| $b$ | 2.91 |
| $C_k$ | 1.2 |
| $e_0$ | 2.5 |
| $k_0$ | $5\times10^{-7}$ mm/s |
| $\mu$ | 100 |

One of the most important issues in consolidation analyses involves the use of laboratory test results on a thin soil specimen to predict the development of strain with time for thick soil layers in the field. It is assumed in general that the time required for a certain degree of consolidation is proportional to the square of the drainage length (Jamiolkowski et al. 1985)

$$\frac{t_H}{t_h}=\left(\frac{H}{h}\right)^2 \tag{31}$$

where $t_H$ and $t_h$ = times required for the same degree of consolidation of a field clay layer and laboratory specimen having drainage distance $H$ and $h$, respectively. Jamiolkowski et al. (1985) considered the above equation as a limiting case of consolidation prediction, and referred to it as Hypothesis-A [Fig. 6(b)]. According to this hypothesis, creep occurs only after the end of primary consolidation, and hence the time required for excess pore pressure dissipation has no effect on the void ratio reduction at the EOP (Mesri and Godleski 1977). On the other hand in Hypothesis-B (Jamiolkowski et al. 1985), the structural viscosity is assumed to cause void ratio reduction even during the excess pore pressure dissipation. Since the time required for excess pore pressure dissipation in the field is more than that of a laboratory sample, the field EOP strain is expected to be higher [Fig. 6(b)].

Fig. 6(a) also shows the predicted strain–time curves based on the result of the 2 cm thick specimen and the proportional law [Eq. (31)]. It can be seen that for a given time the predicted strain using this model is more than that predicted by Eq. (31). Moreover, the strain–time curve of a thick clay layer obtained from

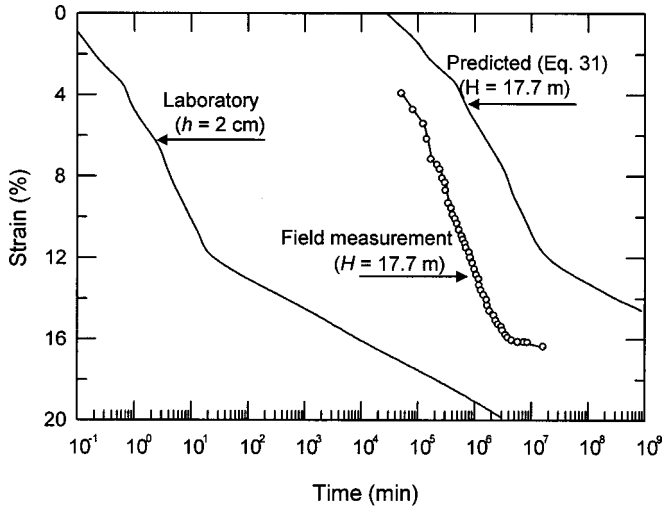


**Fig. 7.** Field performance and prediction of settlement (after Aboshi 1995)

this model does not follow any of the hypotheses (A or B), rather it is in between these two. In addition to the laboratory tests (Aboshi 1973), similar behavior was observed in the field (Aboshi 1995) (see Fig. 7).

Šuklje (1957) analyzed the consolidation process using isotache of consolidation rate and showed that the final strain of a thick soil layer is the same as that of the thin soil sample. However, consideration of yield and structural viscosity in the present model [Eq. 5] resulted in strain in a thick clay that is always less than that of a thin soil layer [Fig. 6(a)].

The location of EOP is usually determined on the basis of different graphical methods, such as Taylor's $\sqrt{t}$ or Casagrande's $\log t$ methods. On the other hand, Mesri and Choi (1985) considered the state of 98% excess pore water pressure dissipation at the impervious boundary as the end of primary consolidation. The strains at the EOP for the different thickness of the specimens were determined using these methods and are plotted in Fig. 8. It

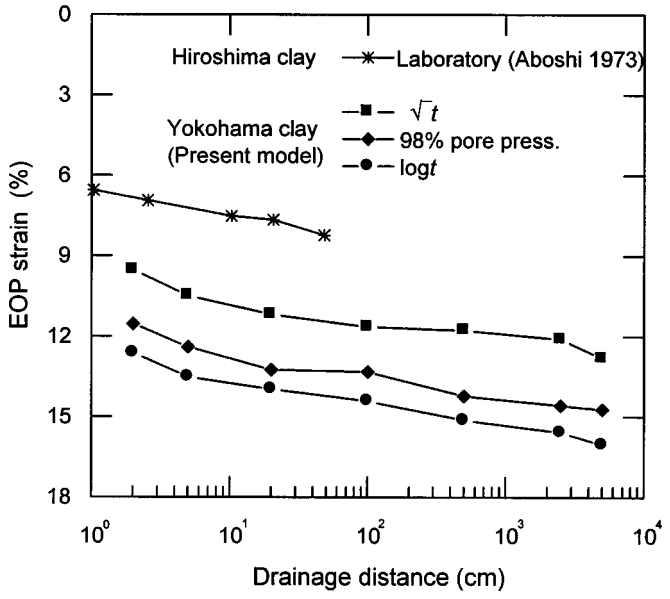


**Fig. 8.** Strain at end of primary consolidation

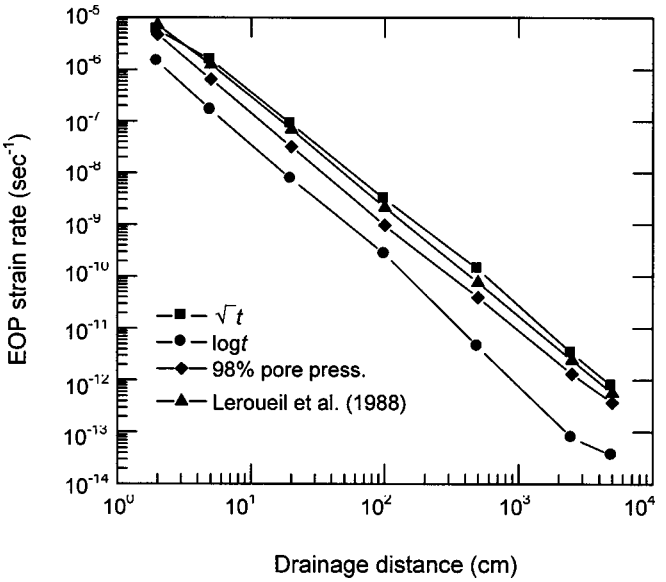


**Fig. 9.** Strain rate at end of primary consolidation

can be seen that the EOP strains obtained by these graphical methods are different. Leroueil et al. (1990) also noted similar difference in these graphical methods. Irrespective of the method used to find the EOP, the strain at the EOP increases with increase in thickness of clay layer. This trend is similar to the experimental results on Hiroshima clay (Aboshi 1973) and marine clays of Tokyo Bay (Murakami 1988). Aboshi's test data is also plotted in Fig. 8 for comparison purposes. The strain at the end of primary consolidation is higher for Yokohama clay than for Hiroshima clay.

## Strain Rate at End of Primary

Strain rate at the end of primary consolidation ($\dot{\varepsilon}_{\mathrm{EOP}}$) for different thickness of clay layer is plotted in Fig. 9. It can be seen that there exists a near linear relationship between $\dot{\varepsilon}_{\mathrm{EOP}}$ and the thickness of the clay layer, when plotted in log–log scale. For these soil layers, $\dot{\varepsilon}_{\mathrm{EOP}}$ calculated from the empirical relation proposed by Leroueil et al. (1988) [$\dot{\varepsilon}_{\mathrm{EOP}}=(0.16ku_0/\gamma_w H^2)$, where $u_0$ is the residual pore pressure and $H$ is the drainage length] is also plotted in Fig. 9. All the predictions show a decrease in EOP strain rate with increase in the thickness of clay layer.

## Coefficient of Consolidation

Fig. 10 shows the coefficient of consolidation ($c_v$) obtained from the result of numerical analyses using Taylor's $\sqrt{t}$ and Casagrande's $\log t$ methods. The value of $c_v$ obtained from $\sqrt{t}$ method is higher than that obtained from $\log t$ method. Using same test data on Champlain clays, Leroueil et al. (1990) also showed similar behavior. Fig. 10 shows that the magnitude of $c_v$ increases with the increase in thickness of the clay layer. This trend is quite similar to the test results on Hiroshima clay (Aboshi 1973).

Based on the above analyses it is therefore suggested to use the laboratory results only to obtain parameters of a numerical model similar to the one presented here. The program may then be used to directly calculate field strains rather than using any of the hypotheses as done in current practice.

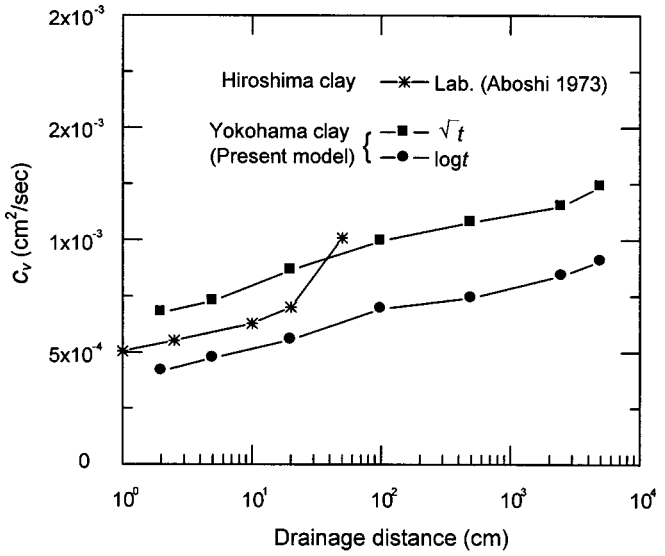


**Fig. 10.** Coefficient of consolidation for different thickness of clay layer

## Preyield Consolidation Behavior

The compression of a clay element during primary consolidation is the resultant effect of effective stress increase and time-dependent viscous action. It has been shown before from our experimental results that a linear relation [Eq. 4] can represent the consolidation behavior of clay elements after yield. Such a relationship, however, does not satisfy the compression behavior before yield. Currently, no reliable methods exist to separate the stress and time effects during the primary consolidation stage. In order to examine these effects two apparent compression indexes are defined as

$$[C_c]_t = [\Delta e/\Delta \log \sigma']_t \tag{32}$$

$$[C_\alpha]_{\sigma'} = [\Delta e/\Delta \log t]_{\sigma'} \tag{33}$$

where $[C_c]_t$ = apparent compression index at time $t$; and $[C_\alpha]_{\sigma'}$ = apparent secondary compression index at a constant effective stress $\sigma'$. Note that the conventional $C_c$ is the slope of 24 h compression line in $e-\log\sigma'$ plot and $C_\alpha$ is the slope of $e-\log t$ curve at secondary consolidation stage which are different from these apparent compression indexes.

Fig. 11 shows void ratio and effective stress change with time for the different subspecimens obtained from interconnected consolidation test for a load increment 1.6→3.2 kg/cm$^2$. The $e-\log\sigma'$ plot for this test was shown in Fig. 2(a). These test results are used to calculate $[C_\alpha]_{\sigma'}$ and $[C_c]_t$ as follows.

In order to get void ratio and effective stress of the subspecimens at time $t_i$, a vertical line is drawn at $t=t_i$ as shown in Fig. 11. The values of effective stress of the different subspecimens at different drainage distances are obtained from the intersections of this line with $\sigma'-\log t$ curves (e.g., for $i$th element $\sigma'=\sigma'_i$). The corresponding void ratios at this time for the different elements are obtained from the $e-\log t$ plot [Fig. 11(a)]. Similarly, in order to obtain void ratio for a constant effective stress $\sigma'_i$ a horizontal line is drawn at the desired effective stress level (e.g., at $\sigma'=\sigma'_i$) [Fig. 11(b)]. Intersections of this line with $\sigma'-\log t$ curves give the time required for the different elements to reach this stress level ($\sigma'_i$). Using these times, the void ratios of the corresponding soil elements are obtained from Fig. 11(a).

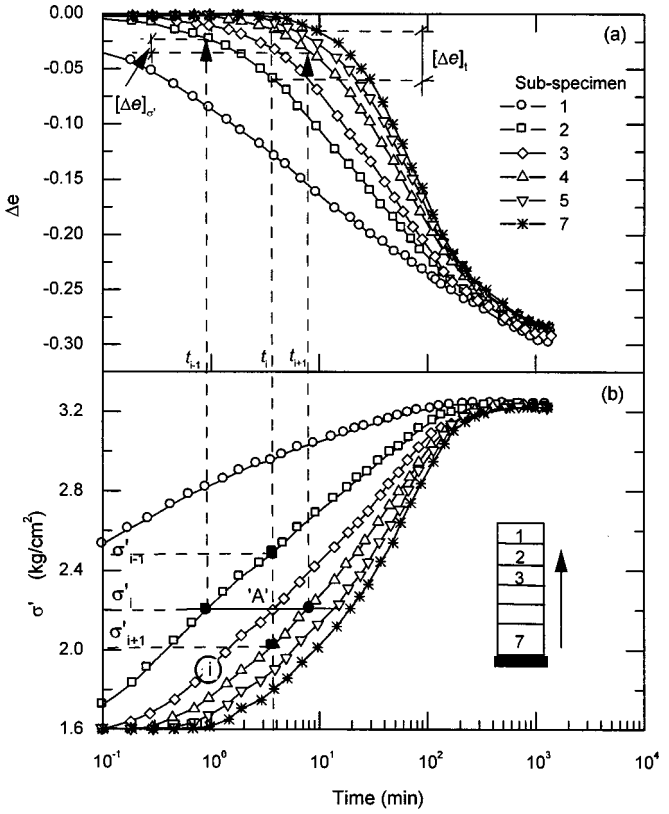


**Fig. 11.** Void ratio and effective stress change in subelements (from interconnected consolidation tests)

With reference to Fig. 11, the values of $[C_c]_t$ and $[C_\alpha]_{\sigma'}$ for the $i$th subelement can be calculated as

$$[C_c]_t = \frac{[\Delta e]_t}{\log\sigma'_{i-1} - \log\sigma'_{i+1}} \tag{34}$$

$$[C_\alpha]_{\sigma'} = \frac{[\Delta e]_{\sigma'}}{\log t_{i+1} - \log t_{i-1}} \tag{35}$$

where $[\Delta e]_t$ and $[\Delta e]_{\sigma'}$ = change in void ratio only due to effective stress change and time, respectively.

The variations of $[C_c]_t$ and $[C_\alpha]_{\sigma'}$ are as shown in Figs. 12 (a and b), respectively. As shown in Fig. 12(a), all of the state points lie above the 24 h compression line during consolidation. Therefore, the stress strain curve cannot be obtained simply by joining the points at 24 h of consolidation as commonly done in practice. The magnitude $[C_c]_t$ is low initially (e.g., at time = 0.1 min) and gradually increases with the progress of consolidation (i.e., time). The reduction of the void ratio under a constant effective stress as shown in Fig. 12(b) is further proof of the contribution of structural viscosity during the excess pore water pressure dissipation. The value of $[C_\alpha]_{\sigma'}$ is very low at the initial stage of consolidation (e.g., $\sigma'=1.65$ kg/cm$^2$) which also increases with the progress of consolidation [Fig. 12(b)]

Mesri and Godleski (1977) have shown that coefficient of secondary compression ($C_\alpha$) is related to coefficient of compression $C_c$. For most clays $C_\alpha/C_c$ was found to be approximately equal to 0.04. In order to examine the relationship between the apparent compression indexes $[C_\alpha]_{\sigma'}$ and $[C_c]_t$ during primary consolidation (i.e., $d\sigma'/dt\neq 0$), they are plotted as shown in Fig. 13. It can be seen that initially the values of both apparent compression indexes are small. However, they increase gradually with time. It

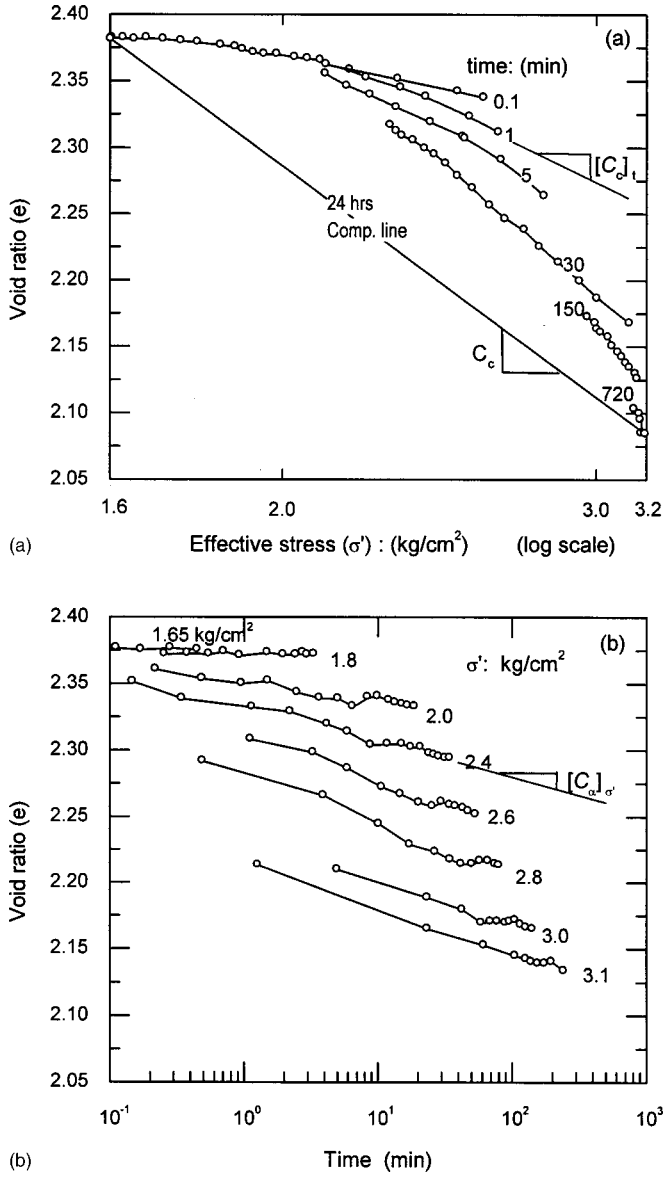


**Fig. 12.** (a) Stress-dependent component of compression; and (b) time-dependent component of compression

is also noted that at a given time, both indexes are higher for elements near the drainage boundary than those for elements near the undrained boundary. Moreover, the ratio $[C_\alpha]_{\sigma'}/[C_c]_t$ is not same as $C_\alpha/C_c$ obtained from conventional one-dimensional consolidation test.

## Nonlinear Model for Preyield Consolidation

The reduction of void ratio during consolidation from preyield to postyield is smooth [Fig. 2(a)]. Therefore, a complete consolidation model must enable a gradual change in compression behavior from preyield to postyield consolidation.

The preyield nonlinear model of deformation used in this study [Eq. (8)] was chosen with the above continuity requirement in mind. In order to demonstrate its effectiveness, consider two other potential preyield models as shown schematically in Fig. 14. In Model A the yield stress of each soil element is assumed to be the same (Murakami 1992) and the $e-\log\sigma'$ relationship is linear

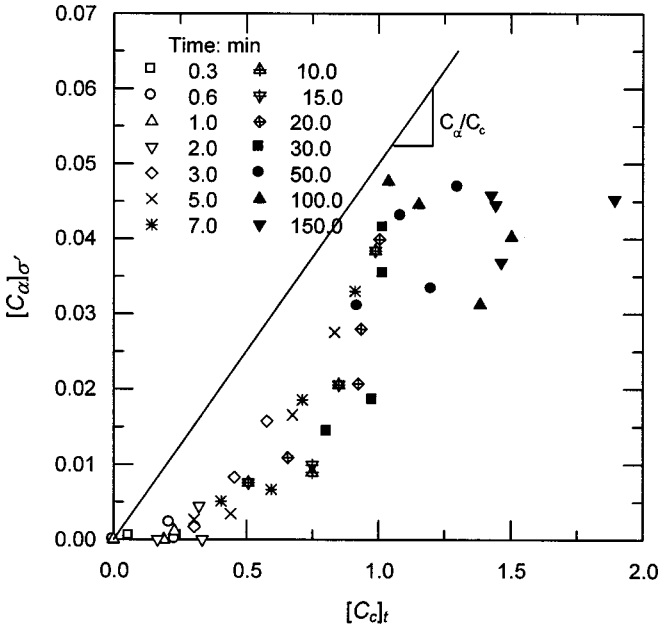


**Fig. 13.** Relationship between apparent compression indexes

before the yield having a slope equal to the swelling index $C_s$. Model B is the same as the Model A except that $e-\log\sigma'$ is nonlinear before yield. At the initial stages of consolidation the slope of $e-\log\sigma'$ is equal to $C_s$ and it attains a slope equal to $C_c$ at the point of yield.

Using the above mentioned models in the program the $e-\log t$ and $\sigma'-\log t$ curves were constructed for a 2 cm thick soil specimen, and then the apparent compression indexes ($[C_c]_t$ and $[C_\alpha]_{\sigma'}$) were determined. The relationship between the apparent compression indexes ($[C_c]_t$ and $[C_\alpha]_{\sigma'}$) in the preyield region is shown in Fig. 15. The performances of the models are very different. According to Model A, $[C_c]_t(=C_s)$ and $[C_\alpha]_{\sigma'}(=0)$ remain constant during the consolidation before yield. In the case of Model B, $[C_c]_t]$ increases with the progress of consolidation but $[C_\alpha]_{\sigma'}$ still remains zero. Since $[C_\alpha]_{\sigma'}$ reflects the effect of viscosity, none of these models can capture the viscous effects in the preyield consolidation process. However, the present model is able to simulate the gradual increase of apparent compression indexes. The rate of change of apparent compression indexes is also higher for the element near the drainage boundary as observed from the laboratory tests (cf. Fig. 13).

## Conclusions

This paper presented a detailed examination of the various issues involved in one-dimensional consolidation process from both experimental results using an interconnected consolidometer and numerical model. The model considered the importance of yield and viscosity throughout the consolidation process. A nonlinear compression index for pre-yield and a linear relationship [$\Gamma$ versus. $\log(-\dot{e})$] for postyield consolidation is used to represent the soil compressibility. Many concepts on consolidation used in the current state of practice have been re-examined in light of the experimental as well as the numerically simulated results and the following conclusions are drawn:

1. Viscous contribution to deformation occurs simultaneously with that caused by effective stress increase during primary consolidation. Its effect is less initially and increases with the progress of consolidation.

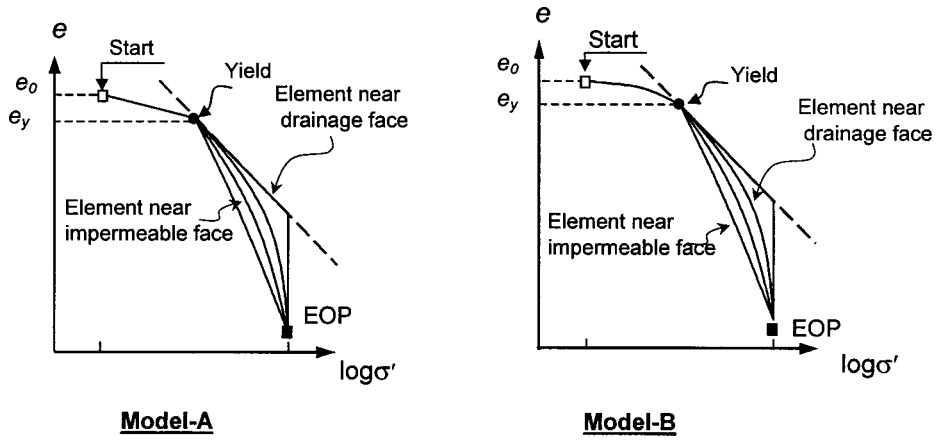


**Fig. 14.** State path followed by different elements

2. The magnitude of yield stress depends not only on the secondary compression during previous loading but also on the drainage distance of the clay element.
3. The void ratio effective stress paths of clay elements depend upon their drainage distance. They do not follow the $e-\log\sigma'$ curve obtained from 24 h reading in the conventional laboratory consolidation test.
4. A linear relationship exists between $\Gamma$ and $\log(-\dot{e})$ during postyield consolidation.
5. Apparent compression indexes $[C_c]_t$ and $[C_\alpha]_{\sigma'}$ increase with the progress of consolidation. The ratio of $[C_\alpha]_{\sigma'}/[C_c]_t$ is not constant.
6. Strain at the end of primary consolidation is not unique. It increases with the thickness of the soil layer. That is, the field EOP strain will be higher than those observed in thin laboratory specimens. The strain rate at EOP decreases with the thickness of clay layer.
7. Coefficient of consolidation ($c_v$) increases with the increase in drainage length.

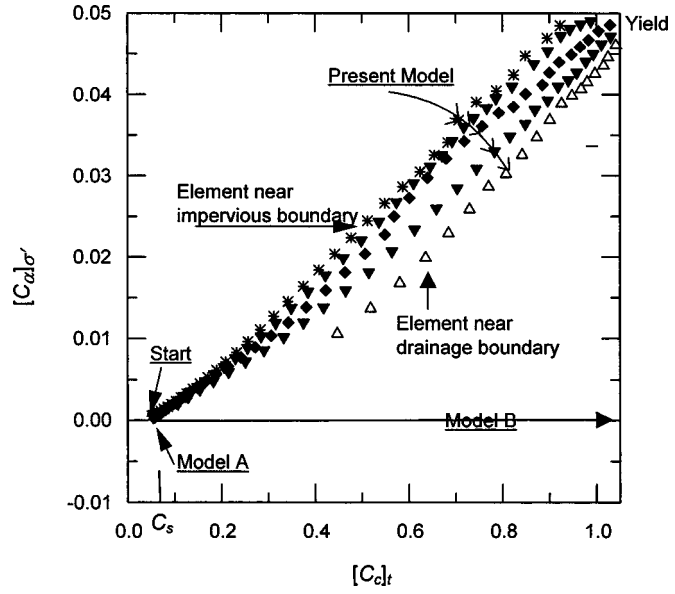


**Fig. 15.** Model prediction of apparent compression indexes

## Acknowledgments

The work presented in this paper is based on the collaborative research at Yokohama National University and at Cambridge Univ. The research in Japan was supported by Grant-in-aid for Scientific Research No. B-2, 08455219 of the Ministry of Education, Science, Sports and Culture, Japan. The second writer acknowledges the International Fellowship Award by the U.S. National Science Foundation (Grant No. INT-9802887) that enabled the collaborative effort at Cambridge University with the first author. Sincere thanks are to Professor K. Y. Lo for his valuable comments during the preparation of this manuscript.

## Notation

*The following symbols are used in this paper:*

$a$ = vertical position in Lagrangian coordinate system;
$C_c$ = compression index;
$C_s$ = swelling index;
$C_\alpha$ = secondary compression index;
$\dot{e}$ = void-ratio rate $(-\Delta e/\Delta t)$;
$e$ = current void ratio;
$e_0$ = initial void ratio;
$H$ = height of clay layer;
$k_v$ = coefficient of vertical permeability;
$k_{v0}$ = initial coefficient of vertical permeability;
$t$ = time;
$U_\varepsilon$ = degree of consolidation from settlement;
$U_{\sigma'}$ = degree of consolidation from pore pressure;
$z$ = vertical position in reduced coordinate system;
$\gamma'$ = submerged unit weight;
$\gamma_s$ = unit weight of soil particles;
$\gamma_w$ = unit weight of water;
$\Delta e^{ir}$ = irrecoverable (plastic+viscous) void ratio change;
$\Delta e^r$ = recoverable (elastic) void ratio change;
$\Delta t$ = time increment; and
$\sigma'$ = effective stress.

## References

Aboshi, H. (1973). ''An experimental investigation on the similitude in the consolidation of a soft clay including the secondary creep settle-

ment.'' *Proc., 8th Int. Conf. on Soil Mechanics and Foundation Engineering*, Moscow, 88.
Aboshi, H. (1995). ''Case records of long-term measurement of consolidation settlement.'' *Key Note Lecture on, Compression and Consolidation of Clayey Soil, IS-Hiroshima*, Vol. 2, Japan, Balkema, Rotterdam, The Netherlands, 847–872.
Crawford, C. B. (1986). ''State of art: Evaluation and interpretation of soil consolidation tests.'' *ASTM Spec. Tech. Publ.*, 892, 71–103.
Gibson, R. E., England, G. L., and Hussey, M. J. L. (1967). ''The theory of one-dimensional consolidation of saturated clays; I Finite non linear consolidation of thin homogeneous layers.'' *Geotechnique*, 17, 261–273.
Hawlader, B. C. (1998). ''Elasto-viscoplastic analysis of one-dimensional consolidation of soft clay.'' PhD thesis, Yokohama National Univ., Yokohama, Japan.
Hawley, J. G., and Borin, D. L. (1973). ''A unified theory for consolidation of clays.'' *Proc., 8th Int. Conf. on Soil Mechanics and Foundation Engineering*, Moscow, 107–119.
Imai, G. (1995). ''Analytical examination of the foundation to formulate consolidation phenomena with inherent time dependence.'' *Key Note Lecture on Compression and Consolidation of Clayey Soil, IS-Hiroshima, Japan*, Balkema, Rotterdam, The Netherlands, 891–935.
Imai, G., and Tang, Y. X. (1992). ''A constitutive equation of one-dimensional consolidation derived from inter-connected tests.'' *Soils Found.*, 32(2), 83–96.
Jamiolkowski, M., Ladd, C. C., Germaine, J. T., and Lancellota, R. (1985). ''New developments in the field and laboratory testing of soils.'' *Proc., 11th Int. Conf. on Soil Mechanics and Foundation Engineering*, San Francisco, 57–153.
Kabbaj, M., Oka, F., Leroueil, S., and Tavenas, F. (1986). ''Consolidation of natural clays and laboratory testing.'' *ASTM Spec. Tech. Publ.*, 892, 378–404.
Leonards, G. A. (1985). ''Discussion of theme lecture 2: New developments in the field and laboratory testing of soils by Jamiolkowski et al.'' *Proc., 11th Int. Conf. on Soil Mechanics and Foundation Engineering*, San Francisco, 2674–2675.
Leonards, G. A., and Altschaeffl, A. G. (1964). ''Compressibility of clay.'' *Trans. Am. Soc. Civ. Eng.*, 90(5), 133–155.
Leroueil, S. (1997). ''Critical state soil mechanics and the behaviour of real soils.'' *Proc., Symp. on Recent Developments in Soil and Pavement Mechanics*, Rio de Janeiro, Brazil, 1–39.
Leroueil, S., Kabbaj, M., and Tavenas, F. (1988). ''Study of the validity of a $\sigma'_v - \varepsilon_v - \dot{\varepsilon}_v$ model in situ conditions.'' *Soils Found.*, 28(3), 13–25.
Leroueil, S., Kabbaj, M., Tavenas, F., and Bouchard, R. (1985). ''Stress-strain-strain rate relation for the compressibility of sensitive natural clays.'' *Geotechnique*, 35(2), 159–180.
Leroueil, S., Magnan, J. P., and Tavenas, F. (1990). *Embankments on soft clays*, Ellis Horwood.
Mesri, G., and Choi, Y. K. (1979). ''Discussion on strain rate behaviour of St. Jean Vianney clay.'' *Can. Geotech. J.*, 16(4), 831–834.
Mesri, G., and Choi, Y. K. (1985). ''The uniqueness of the end-of-primary (EOP) void ratio-effective stress relationship.'' *Proc., 11th Int. Conf. on Soil Mechanics and Foundation Engineering*, San Francisco, 587–590.
Mesri, G., and Godleski, R. M. (1977). ''Time and stress compressibility interrelationship.'' *J. Geotech. Eng.*, 103(5), 417–430.
Mesri, G., Shahien, M., and Feng, T. W. (1995). ''Compressibility parameters during primary consolidation.'' *Proc., Compression and Consolidation of Clayey Soils, IS-Hiroshima, Japan*, Vol. 2, Balkema, Rotterdam, The Netherlands, 1021–1037.
Mitchell, J. K. (1976). *Fundamentals of soil behaviour*, Wiley, New York.
Murakami, Y. (1988). ''Secondary compression in the stage of primary consolidation.'' *Soils Found.*, 28(3), 169–174.
Murakami, Y. (1992). ''Quasi-preconsolidation effects developed in normally consolidated clays.'' *Soils Found.*, 32(4), 171–177.
Scott, R. F. (1963). *Principles of soil mechanics*, Addison-Wesley, Reading, Mass.
Šuklje, L. (1957). ''The analysis of consolidation process by isotache method.'' *Proc., 4th Int. Conf. on Soil Mechanics and Foundation Engineering*, Vol. 1, London, 200–206.
Tan, T. S., and Scott, R. F. (1988). ''Finite strain consolidation—A study of convection.'' *Soils Found.*, 28(3), 64–74.
Tavenas, F., Jean, P., Leblond, P., and Leroueil, S. (1983). ''The permeability of natural clays, Part II: Permeability characteristics.'' *Can. Geotech. J.*, 20(4), 645–660.
Terzaghi, K. (1923). ''Die Berechnung der durchlassigkeit des tones aus dem Verlauf der hydrodynamischen Spnnungserscheinungen.'' *Akad. der Wiss., Wien, Sitzungsberichte, Mathematisch Naturwissenschaftliche Klasse*, 132(3–4), 125–138.
Thomas, J. W. (1995). *Numerical partial differential equations: Finite difference methods*, Springer, New York.
Yin, J. H., and Graham, J. (1989). ''Viscous-elastic-plastic modeling of one-dimensional time-dependent behavior of clays.'' *Can. Geotech. J.*, 26(2), 199–209.